ASEAN
Journal of Scientific and Technological Reports
Online ISSN:2773-8752

Research article

Sustainable Construction with Cost-effective High-performance Building Materials: Utilizing Natural Activated Carbon Nanofillers Reinforced HDPE Nanocomposite

Mousam Choudhury[1, 5], Jagjiwan Mittal[2], Somnath Chanda Roy[3], and Ranu Nayak[4*]

[1] Amity Institute of Nanotechnology, Amity University, Noida, Uttar Pradesh, India
[2] Amity Institute of Nanotechnology, Amity University, Noida, Uttar Pradesh, India
[3] Department of Physics, Indian Institute of Technology, Madras , India
[4] Amity Institute of Nanotechnology, Amity University, Noida, Uttar Pradesh, India
[5] Central Institute of Petrochemicals Engineering & Technology (CIPET), CSTS Aurangabad, Maharashtra, India
* Correspondence: rnayak@amity.edu

Citation:
Choudhury, M.; Mittal, J.; Roy C.S.; Nayak, R. Sustainable construction with cost-effective high-performance building materials: utilizing natural activated carbon nanofillers reinforced HDPE nanocomposite. *ASEAN J. Sci. Tech. Report.* **2025**, *28*(2), e256339. https://doi.org/10.55164/ajstr.v28i2.256339

Article history:
Received: October 16, 2024
Revised: December 30, 2024
Accepted: January 30, 2025
Available online: February 23, 2025

Abstract: This study explores the development of HDPE nanocomposites reinforced with low-cost, naturally derived activated nanocarbon (ACN) fillers, providing an alternative to conventional carbon nanotube (CNT)-reinforced HDPE, which, despite its superior properties, remains expensive and complex to fabricate. ACN-HDPE nanocomposites were fabricated at varying filler loadings (2 wt.%, 5 wt.%, and 10 wt.%) and systematically compared with CNT-HDPE counterparts (1 wt.% and 2 wt.%) across multiple performance metrics. These included mechanical strength (tensile strength, impact strength, flexural stress, compressive strength, and elongation at break), thermal stability (heat deflection temperature, vicat softening point, and oxidative induction time), flammability (vertical burn tests), and weather resistance (UV/moisture aging and gas permeability). The results demonstrate that 10 wt.% ACN-HDPE composites achieved a 161% increase in impact strength and substantial improvements in other mechanical parameters. Thermal properties were markedly enhanced, with a 51% increase in heat deflection temperature, a 39% rise in Vicat softening point, and a remarkable 426% extension in oxidative induction time. Flammability resistance improved by 93%, while UV/moisture degradation and gas permeability were reduced by 12% and 60%, respectively. These composites performed comparably to 2 wt.% CNT-HDPE in all evaluated aspects, emphasizing their viability for high-performance applications. With enhanced mechanical, thermal, and flame-retardant properties, ACN-HDPE nanocomposites offer a cost-effective, eco-friendly alternative to CNT-HDPE and pristine HDPE. These materials present a transformative solution for sustainable construction, delivering high performance while significantly reducing costs and environmental impact.

Keywords: HDPE building material; Carbon nanotube; Activated nanocarbon; Polymer nanocomposites; Reinforcement

1. Introduction

The building and construction are critical to global development and major energy consumers. The construction industry is transforming to stay competitive,

focusing on enhancing quality, reducing waste, and improving recyclability. Emerging alternatives are challenging traditional materials like brick, concrete, and steel due to their limitations in versatility and aesthetics. For instance, wood, known for strength and durability, is increasingly being replaced by polymers due to its susceptibility to decay, fire, termites, and weather damage [1]. Similarly, alternative materials such as cement, brick, natural earth, and bamboo are susceptible to similar hazards like fire, weather, and moisture [2]. Steel, although strong, is costly and prone to rusting [3]. Polymers, particularly HDPE and CPVC, are gaining popularity as sustainable, cost-effective alternatives [4]. HDPE is favored for its flexibility, weather resistance, and durability, making it ideal for pipelines and other applications requiring adaptability to extreme conditions. HDPE composites, enhanced by micro and nanofillers like carbon black, activated carbon, and graphene, exhibit improved mechanical and thermal properties. Although carbon nanomaterials like carbon nanotubes (CNTs) deliver superior performance, their high cost and challenges with recyclability limit their widespread adoption.

Different variants of polymers are emerging as an affordable, sustainable, and robust alternative for residential construction [4]. Chlorinated polyvinyl chloride (CPVC) [5] and HDPE are popular among these variants. The production of CPVC doors and window frames is gaining popularity over traditional wooden doors and windows due to their high-pressure sustainability. However, CPVC exhibits brittle behavior and lower chemical resistance. On the other hand, HDPE can withstand higher pressure, is much more flexible, chemically resistant, and has a longer service life without degradation [6–8]. Being flexible, HDPE is better suited to curved pipeline systems. Moreover, HDPE is highly UV resistant and can be installed under extreme temperatures conditioned between -40°C to 140°C. These attributes position HDPE as a promising material for modern construction practices. Traditional construction materials often come with high costs and maintenance. In contrast, HDPE plastics offer unmatched flexibility, weather resistance, and adaptability, making them increasingly popular in modern construction [9]. HDPE's cost-effectiveness and versatility position it as a key material for future construction practices, especially due to its chemical resistance and environmental friendliness. HDPE composites are like carbon, becoming essential, with property enhancements achieved by incorporating micro and nanofillers.

Thermal, mechanical, and tribological properties of HDPE matrices have been significantly enhanced using carbon microfilters like carbon black [10, 11], microdimensional activated carbon from rice husk [12, 13], corn stalk, and fly ash [14]. Advanced nanofillers such as carbon nanotubes (CNT) [15–20] and graphene [21], along with hybrid CNT-alumina [22] and graphene-alumina nanoparticles [23], offer exceptional property improvements with low filler content [24, 25]. However, their high manufacturing costs and potential complications in recycling remain drawbacks [26, 27].

Research on low-cost activated carbon microfilters derived from agricultural wastes, such as rice husk and cork stalk, demonstrates moderate improvements in HDPE's flexural properties and flame retardancy [12, 13]. Compounding carbon black (2 wt.%) with HDPE under high humidity enhanced mechanical properties, including impact resistance and elongation [10]. Similarly, blending HDPE with biochar from biomass sources, such as olive tree pruning or Ayous sawdust, has shown moderate to significant improvements in thermal stability, elasticity, and mechanical strength, depending on filler loading [28, 29]. Some extensive studies involved investigating the performance of various carbon nanofillers (1D, 2D, and 3D), including graphene, CNT, fullerene, carbon black, nanodiamond, and reduced graphene oxide with HDPE [30, 31]. In one of these studies, interesting key findings included a 30% to 40% increase in impact strength of HDFC after using fillers like carbon black, nanodiamonds, fullerene, and CNT, whereas a decrease of 25% to 30% for 3D plate-like nanofillers [31]. HDPE micro-and nanocomposites with varying contents of hybrid inorganic micro and nanofillers of $CaCO_3$ and fumed silica improved HDPE's mechanical properties, thermal stability, and melting temperature impressively [32]. While nanocarbon fillers like CNTs and graphene significantly enhance HDPE's performance, their high cost and environmental concerns highlight the need for sustainable alternatives.

This study addresses these challenges by fabricating HDPE composites reinforced with low-cost activated nanocarbon fillers derived from natural sources. This sustainable approach aims to produce high-performance interior building materials with improved or comparable mechanical and thermal properties, weatherability, and flame resistance to CNT-reinforced HDPE composites. By leveraging activated

nanocarbon fillers, this research advances the development of smarter and more sustainable construction practices aligned with global sustainability goals.

2. Materials and Methods

2.1 Materials

HDPE, with a density of 0.95 g/cm³ (measured at 23°C according to ASTM D1505), was sourced from Haldia Petrochemicals, India, under the trade name Halene-H™ M5018L. Activated nanocarbon powder (ACN) with 99.9% purity and particle size ranging between 60 nm to 100 nm, derived from coconut shell and having a bulk density of 0.28 g/ml, was obtained commercially from Nanoshel, India. Multiwalled carbon nanotubes (CNTs) (99% purity, diameter: 10-20 nm, length: 3-8 μm) were also procured from Nanoshel, India. A detailed specification sheet of these commercial raw materials is given in the supporting information. IGEPAL CO630, a non-ionic detergent used for stress-cracking evaluation of building materials, was used without modification.

2.2 Fabrication of Carbon-based HDPE Nanocomposite

ACN-HDPE and CNT-HDPE nanocomposites and virgin HDPE were melt-blended at optimal ratios with varying weight percentages of carbon nanofillers. At a processing window of 190°C, the matrix and fillers were processed with a barrel temperature of 180°C at the feed zone to compression zones at 190°C and 195°C and maintained at 195°, 200°, 200°, and 205°, till the metering zone of exit of the twin screw extruder. The extrusion nozzle temperature was maintained at 230°C to 235°C with a deviation of ± 5°C temperature with a screw speed of 200 rpm and a throughput of 1 kg/h, resulting in a residence time of about 55 s. Formulations included ACN at 0 wt.%, 2 wt.%, 5 wt.%, 10 wt.%, and 20 wt.% and CNT at 0 wt.%, 1 wt.%, and 2 wt.% in the HDPE matrix. The extruded mixtures were pelletized using a Thermo Scientific extruder, pre-dried, and processed into sheets and test specimens via injection molding under constant temperature conditions. Test samples were prepared using four-cavity molds per ASTM standards and labeled as ACN2, ACN5, ACN10, ACN20 (for 2/5/10/20 wt.% ACN-HDPE) and CNT1, CNT2 (for 1/2 wt.% CNT-HDPE), with pristine HDPE denoted as PT.

2.3 Melt Flow Rheology

Melt flow index (MFI) for rheological property evaluation was conducted at 190 °C with a 2.1 kg load and was performed as per ASTM D1238.

2.4 Structural and Surface Morphology Analysis

Surface study of fractured surfaces of composites was done using the F-50 general-purpose field-emission Scanning Electron Microscope instrument (FESEM) JEOL7001 using a beam energy of 15 KeV. Bruker D2 phaser X-ray diffractometer was used to measure the X-ray diffraction peaks of the composite surface for all the formulations. The diffraction angle 2θ ranged from 10° to 60° with a scan increment of 0.02°.

2.5 Thermal Property

2.5.1 Thermal Conductivity

Thermal conductivity was assessed in nanocomposite samples (2, 5, 10 wt.% ACN and 1, 2 wt.% CNT loaded HDPE, 50 mm diameter each) using a Guarded Hot Plate (Anter Corporation, Model 2022). Samples were heated on one side by an electrically heated plate and cooled on the opposite side, with temperature differences recorded via in-built thermocouples. Thermal resistivity and mean sample temperatures were analyzed using software version 5.0.

2.5.2 Heat Distortion Temperature (HDT) and Vicat Softening Temperature (VST)

For HDT, specimens (pristine HDPE, ACN-HDPE, CNT-HDPE) were prepared per ASTM D648 (5" × ½" × ¼"), placed in an HDT apparatus, and subjected to a 0.45 MPa load. Immersed in a silicone oil bath, the temperature was raised at 2°C/min until a 0.25 mm deflection occurred, recording the temperature. For VST, 3 mm thick, 10 mm square specimens were tested using a VST apparatus. A 10N load was applied, and the

sample was heated in an oil bath at 23°C, increasing at 50°C/hour until the needle penetrated 1 mm. The softening temperature was then recorded in °C.

2.6 Mechanical Characterization

2.6.1 Tensile Strength and Elongation (on Universal Testing Machine)

Test specimens were prepared via injection molding using a 210 T machine and molds, following ASTM D4101 standards. Tensile strength testing was conducted at a 50 mm/min yield rate per ASTM D638. Weatherability tests were performed before tensile strength and elongation evaluations. For accurate strain measurement up to 0.3% extension, three specimens of each formulation were tested using an axial extensometer with a 25 mm gauge length positioned at the center of the samples.

2.6.2 Flexural Stress

Flexural stress, modulus of rupture or bend strength, denotes the maximum stress experienced within a material during rupture. Flexural strength was tested per three-point bending stress on the samples (3 samples for each formulation) prepared as per ASTM D4101 standard. The rectangular bar specimens were tested for flexural modulus as per ASTM D790 (A) standard.

2.6.3 Compressive Strength Test

The compressive strength test evaluates a material's load-bearing capacity under compression, commonly applied to construction materials like bricks and cement. For this study, compressive stress and forces were measured on three samples of each formulation, prepared per ASTM D695-2015 standards, to assess the behavior of ACN-HDPE and CNT-HDPE nanocomposites under a uniform compressive load. Specimens were shaped into blocks (12.7 × 12.7 × 25.4 mm) and cylinders (12.7 mm diameter × 25.4 mm length).

2.6.4 Impact Test

The samples (3 for each formulation) were notched for stress concentration in one place. These notched impact specimens (with a minimum triplicate average) have been tested as per ASTM D256 (A) standard and at room temperature.

2.7 Flammability Test

2.7.1 Relative Flammability

ACN-HDPE, CNT-HDPE, and PT specimens (125 mm × 13 mm × 3 mm) were tested per ASTM D635 to determine relative burning rates, assessing fire behavior without defining fire hazard criteria. PT, ACN2, ACN5, ACN10, CNT1, and CNT2 were tested in vertical and horizontal orientations in a test chamber. Each was exposed to a Bunsen burner flame for 5 seconds. Flame propagation time and distance were recorded until the flame self-extinguished or reached a set distance. The linear burning rate was calculated in mm/min.

2.7.2 Limiting Oxygen Index

The samples' Limiting Oxygen Index (LOI) was determined according to ASTM D2863. HDPE nanocomposites were cut into 150 mm × 10 mm × 4 mm pieces and placed vertically in a glass chimney within an oxygen/nitrogen environment, with the flow starting at the base of the chimney. The top of the sample is ignited, and the oxygen concentration is gradually reduced until the flame is no longer sustained.

2.7.3 Oxidation Induction Time

The thermal stability of pristine HDPE, ACN-HDPE, and CNT-HDPE nanocomposites was assessed using differential scanning calorimetry (DSC). Samples (15–20 mg) were heated in a nitrogen atmosphere above their melting point and then exposed to oxygen at isothermal conditions to induce oxidation. Oxidation induction time (OIT)—the interval between melting and the onset of oxidative decomposition—was measured. Results were averaged across five samples per formulation.

2.8 Weatherability Testing

2.8.1 Accelerated ageing test (using ASTM D4329, ASTM D 4587)

UV aging tests were conducted on CNT- and ACN-loaded HDPE nanocomposites to correlate accelerated weathering with outdoor exposure per ASTM D4329 and ASTM D4587 standards. Five samples of each formulation (3 × 12 inches) were exposed to UV radiation using UVA-340 lamps in a QUV accelerated

weathering tester. Each exposure cycle included 8 hours of UV radiation at 60°C and 4 hours of condensation at 50°C, totaling 504 hours over 21 days. Moisture was applied via forced condensation, with controlled temperatures throughout. After aging, the strength retention of the samples was evaluated using a Universal Testing Machine.

2.8.2 Environmental Stress Cracking Resistance (ESCR) test (as per ASTM D1693)

PT, ACN2, ACN5, ACN10, CNT1, and CNT2 samples were molded into 38 mm × 13 mm specimens, with three per formulation. Internal stress was relieved by boiling the samples in water. Each specimen was notched with a 19 mm cut to create a surface defect, then bent into U-shapes and secured in grooved clamps. The specimens were immersed in test tubes filled with IGEPAL CO630, a stress-cracking chemical. Specimens were then sealed and placed in a constant-temperature bath at 50°C for up to 360 hours, with environmental stress cracking failure observations.

2.8.3 Gas Permeability Test

The test specimens—PT, ACN2, ACN5, ACN10, CNT1, and CNT2—were prepared with a diameter of 100 mm and thickness of 2.5 μm, ensuring they were free of wrinkles, creases, pinholes, and other imperfections, with uniform thickness. Three samples from each formulation were pre-conditioned at 23±2°C in a desiccator over calcium chloride for 48 hours, following ASTM D618. After conditioning, the samples underwent a permeability test for 31 days at a constant oxygen gas flow rate. The volume-flow rate (in μL/s) of transmitted gas was measured to evaluate each sample's gas (oxygen) permeability factor.

3. Results and Discussion

3.1 Fabrication & Physico-chemical Characteristics of HDPE Nanocomposites

The nanocomposite fabrication method significantly impacts filler dispersion and nanoparticle-matrix interaction [27]. This study used co-extrusion with a twin-screw extruder and injection molding without adding surface modifiers. A color change indicated a homogeneous composite formation. Based on previous literature, CNT filler content was limited to 2 wt.% to avoid dispersion issues [33], while ACN fillers were tested up to 20 wt.%. However, the 20 wt.% ACN caused high melt viscosity, complicating extrusion and resulting in non-uniform fabrication, so it was excluded from further studies. Figure 1(a) shows digital images of pristine HDPE and HDPE nanocomposites with varying ACN (2 wt.% to 10 wt.%) and CNT (1 wt.% and 2 wt.%) loadings, all with uniform physical appearance. The fabricated specimens were then analyzed for their physico-chemical properties.

3.1.1 Surface Morphology

Cross-sectional SEM images were used to assess filler distribution in the HDPE matrix. Figure 1(b) shows pristine HDPE with polymer layers and no fillers. The image shows smooth polymer layers with no visible filler material. SEM images in Figure 1(c) reveal dense CNT networks with diameters ranging from 20-30 nm and lengths of 3-8 μm, indicating a high aspect ratio, which suggests potential for mechanical reinforcement. Figure 1(d) displays the cross-section of CNT-HDPE nanocomposites, showing uniformly dispersed CNT bundles throughout the polymer matrix, essential for enhancing thermal and mechanical properties. Figure 1(e) highlights the porous architecture of ACN fillers, with surface roughness ranging from 40-70 nm, providing a larger interfacial area for interaction with the HDPE matrix. This porosity improves the thermal and mechanical properties of the composite. Figure 1(f) shows ACN-HDPE composites with a smoother surface than CNT-HDPE composites. SEM images in Figures 1(d) and 1(f) confirm consistent filler dispersion, improving material homogeneity. This surface morphology study demonstrates that CNT and ACN fillers significantly modify the HDPE matrix, with ACN offering smoothness and filler-matrix integration advantages.

3.1.2 XRD Analysis

XRD spectra (Figure 2) were obtained for pristine HDPE, and the CNT and ACN compounded HDPE nanocomposites. Pristine HDPE exhibited two firm peaks at 21.8° and 24°, corresponding to its orthorhombic unit cell structure's (110) and (200) reflecting planes. An epaulet peak was also observed at 19.8°. Other weaker peaks at 30°, 36.3°, and 41° corresponded to the (210), (020), and (011) planes, respectively. For the CNT and ACN filled HDPE nanocomposites, no distinct peaks were observed for the fillers. However, all peaks shifted

to a lower 2θ angle by approximately 1.5%. The degree of crystallinity (χ_c) was estimated using Origin software, calculated as the ratio of the sum of the deconvoluted crystalline part over the sum of the crystalline and amorphous parts. The crystallinity of HDPE increased from 77% to 79.2% for CNT2 and 77% to 89.7% for ACN10. This increase in crystallinity was attributed to a shift from homogeneous to heterogeneous nucleation, which enhanced the nucleation process and led to more crystalline grains.

3.1.3 Melt Flow Rheology

Figure 3(a) shows that the incorporation of carbon-based nanofillers into HDPE results in a decrease in the MFI as the nanofiller concentration increases. The MFI, a key parameter indicating the flowability and processability of polymer melts, was highest for pristine HDPE (0.743 g/10 min), indicating superior flow and ease of processing due to its unmodified crystalline structure. As ACN fillers were added, MFI decreased progressively with increasing filler content, from a 2% reduction at 2 wt.% ACN to a 30% reduction at 10 wt.% ACN. This reduction in MFI is attributed to enhanced filler dispersion and interaction with the polymer chains, which restricts chain mobility. At higher filler loadings, the formation of nanostructured networks increases melt viscosity, further reducing flowability. The addition of CNT fillers resulted in a more significant decrease in MFI (60-68%) with just 1-2 wt.% loading compared to ACN fillers. This sharp reduction is due to the higher aspect ratio of CNTs, which form a stronger network with the polymer matrix, significantly increasing the melt viscosity and resisting polymer chain mobility due to the rigid, tubular structure of CNTs. ACN10 (0.516 g/10 min) exhibited better flowability than CNT2 (0.236 g/10 min), likely because ACN's smaller aspect ratio and porous structure impose less resistance to polymer chain movement. The MFI trends indicate that ACN-HDPE composites maintain a better balance between processability and performance than CNT-HDPE composites, making them a more cost-effective option for applications where flowability is crucial. Conversely, CNT-HDPE composites are more suited for applications prioritizing mechanical reinforcement and structural integrity. Figure 3(b) demonstrates that pristine HDPE has a 950 kg/m^3 density, attributed to the tightly packed ethylene monomers resulting from crystallization. Upon incorporating nanofillers, the density of the HDPE nanocomposites showed minimal changes. The minimal impact on density can be attributed to the small fraction of nanofillers in the composite, which did not appreciably alter the overall density and effective dispersion of nanofillers within the HDPE matrix without creating voids or defects. ACN10 showed a slight 1% increase in density, likely due to the higher filler loading, contributing to a marginally denser structure. These findings suggest that nanofiller incorporation, particularly at low to moderate loadings, can improve composite performance without significantly affecting the density, thus preserving the lightweight advantages of HDPE.

3.2 Thermal Stability

The thermal stability of the building composites was assessed by comparing PT, ACN2, ACN5, ACN10, CNT1, and CNT2 in terms of heat distortion temperature and composite softening temperature. Strong interfacial interactions between the polymer and nanofiller often improve thermal stability.

3.2.1 Thermal Conductivity

This study's pristine HDPE (PT) exhibited a thermal conductivity of 0.16 W/mK, consistent with its insulating properties. The incorporation of carbon-based nanofillers, such as ACN and CNT, enhanced the thermal conductivity of the HDPE matrix as they are known to possess higher average thermal conductivities of approximately 0.6 W/mK (ACN) and 15 W/mK (CNT) at room temperature [34]. The high thermal conductivity of carbon-based materials arises from their efficient lattice vibrations within the carbon structures, which facilitate superior heat transfer compared to the amorphous HDPE polymer matrix. The experimental results showed a trend of increased thermal conductivity (Table 1) with the addition of carbon fillers in the HDPE matrix. ACN-HDPE composites exhibited a 34% to 46% increase in thermal conductivity, while CNT-HDPE composites demonstrated an enhancement ranging from 34% to 38%.

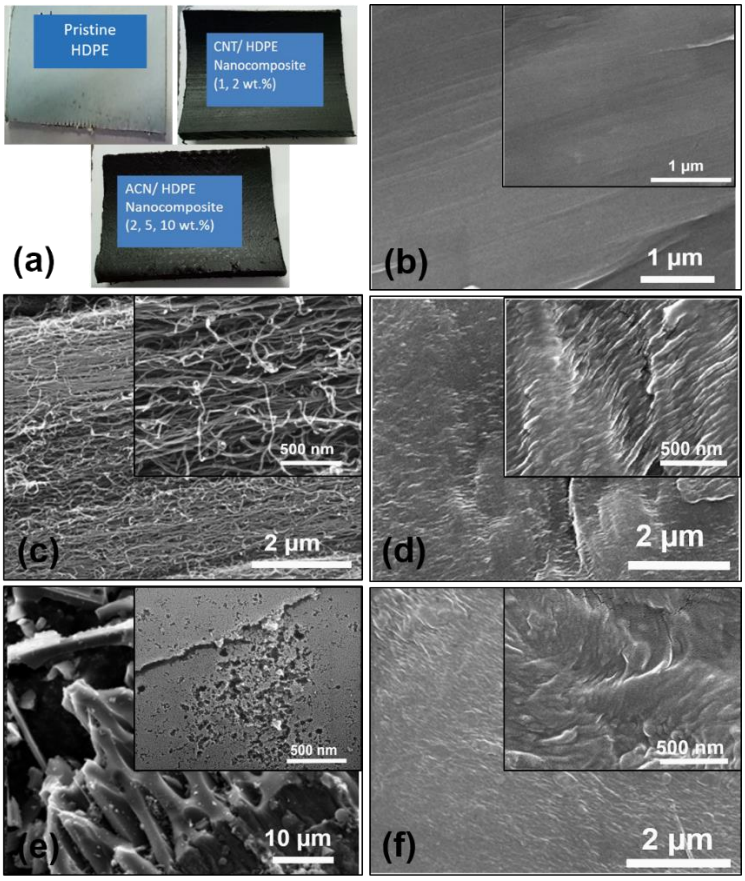

Figure 1. (a) Digital images of pristine HDPE and CNT-HDPE and ACN-HDPE nanocomposites; Cross-sectional SEM images of (b) Pristine (c) CNT filler (d) CNT-HDPE nanocomposite (e) ACN nanofiller; and (f) ACN-HDPE nanocomposite (Note: insets are magnified images)

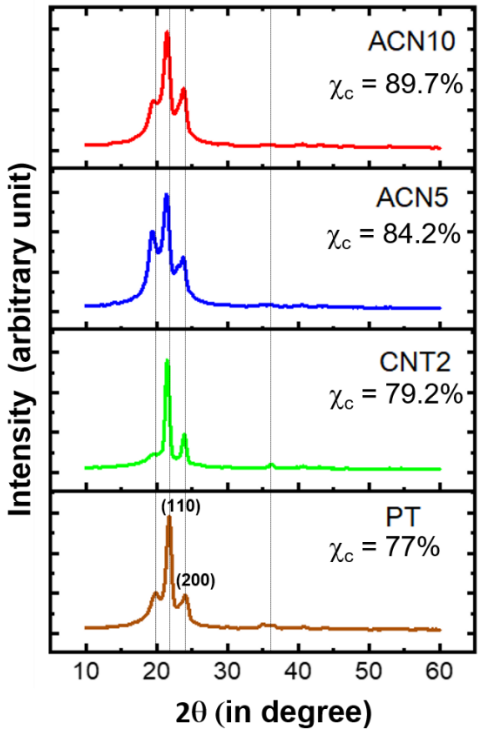

Figure 2. XRD spectra and a corresponding degree of crystallinity (χ_c) for pristine HDPE and CNT-HDPE and ACN-HDPE composites

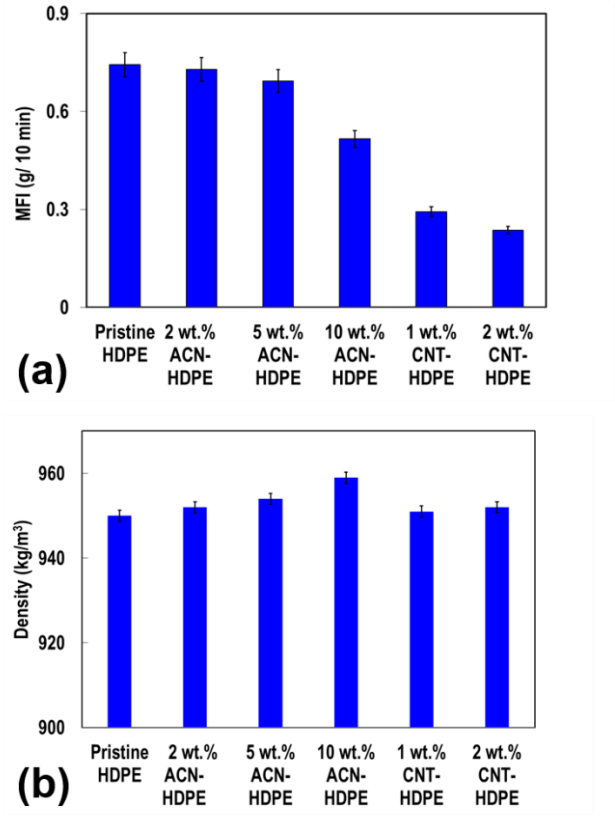

Figure 3. (a) Melt Flow Index (MFI) and (b) density of ACN and CNT loaded HDPE nanocomposites with various filler concentrations

Table 1. Thermal conductivity comparison of HDPE polymer with its carbon nanofiller-loaded nanocomposites

Carbon HDPE nanocomposites	Mean temperature (°C)	Thermal resistance (m^2K/W)	Thermal conductivity (W/mK)
PT	35	11.25×10^{-3}	0.162
ACN2	35.7	8.26×10^{-3}	0.218
ACN5	36.4	7.51×10^{-3}	0.237
ACN10	36.1	7.46×10^{-3}	0.247
CNT1	35.7	8.18×10^{-3}	0.218
CNT2	35.8	8.26×10^{-3}	0.224

Specifically, ACN10 demonstrated 46% improvement, reaching the highest figure at 0.247 W/mK. This increase is attributed to the higher volume fraction of ACN, which forms continuous conductive pathways, improving phonon transfer. Despite CNT's inherently higher thermal conductivity, the relatively low filler content (1 to 2 wt.%) limited the enhancement compared to ACN-HDPE. The reduced thermal resistance supports the increased thermal conductivities of all the composites, indicating improved heat transfer efficiency.

3.2.2 Heat Deflection and Vicat Softening Temperature

HDT (Heat Deflection Temperature) and VST (Vicat Softening Temperature) are key indicators of a material's heat resistance and thermal stability. HDT measures the temperature at which a material begins to deform under load, while VST assesses its ability to maintain its chemical structure at high temperatures. It is observed from Table 2 that incorporating 5 wt.% and 10 wt.% ACN fillers into an HDPE matrix increased the HDT by 48% and 51%, respectively. Adding 1 wt.% and 2 wt.% CNT resulted in HDT increases of 44% and 52%, respectively. VST rose from 67°C for PT to 85°C and 93°C for ACN5 and ACN10, respectively, reflecting a 27% to 39% increase. A 40% rise in VST was observed for CNT2-HDPE. The increase in VST and HDT is similar for both composites. The higher VST is due to greater crystallinity and melting point from the organic

nanofillers, which enhances rigidity and reduces softening, as confirmed by impact test results.

Overall, the increased HDT and VST in ACN-HDPE and CNT-HDPE nanocomposites indicate improved thermal stability and heat resistance, attributed to the nanofillers' role in restricting polymer chain movement and resisting deformation at higher temperatures [35].

Table 2. Thermal properties of pristine HDPE, ACN-HDPE, and MWNT-HDPE nanocomposites

Carbon HDPE nanocomposites	HDT (°C)	VST (°C)
PT	72	67
ACN2	94	84
ACN5	107	85
ACN10	109	93
CNT1	104	92
CNT2	110	94

3.3 Mechanical Characterization

3.3.1 Tensile Strength

Figure 4(a) illustrates the ultimate tensile strength (UTS) of pristine HDPE (PT) and its nanocomposites. Pristine HDPE has a UTS of 16.7 MPa, which serves as the control value. Incorporating nanofillers enhances the tensile strength, with ACN10 showing a 61% increase and CNT2 a 65% improvement over pristine HDPE. This enhancement is attributed to the nanofillers' high surface area and aspect ratio, which facilitate effective stress transfer and uniform dispersion within the polymer matrix. These fillers also act as nucleating agents, promoting improved crystallinity in the HDPE matrix, as confirmed by SEM and XRD analyses. The increased crystallinity enhances tensile strength, thermal stability, and mechanical performance. The carbon-filled nanocomposites outperform pristine HDPE, making them promising for high-performance building materials where enhanced load-bearing capacity and durability are crucial. This aligns with the growing demand for advanced, lightweight, and durable construction materials in modern infrastructure.

3.3.2 Elongation

As depicted in Figure 4(b), ACN5 and ACN10 nanocomposites exhibit higher elongation to break compared to PT and ACN2. Equally, CNT1 and CNT2 display a sharp increase in elongation at break. ACN10 and CNT2 formulations outperformed the other formulations with remarkable enhancement in elongation at the break by 88% and 91%, respectively. The elevated elongation behavior of these nanocomposites can be attributed to the presence of nano-dimensional fillers. Nanomaterials possess greater stress-withholding/absorbing capacity, transferring less stress to the polymer chains. Consequently, they can sustain longer elongation before reaching the breaking point.

3.3.3 Flexural Stress

Flexural stress analysis reveals the bending behavior of HDPE nanocomposites with varying ACN and CNT filler loadings. This is important for evaluating construction materials like beams and joists. Figure 4(c) shows that flexural strength increases with optimal concentrations of these fillers. ACN filler concentration from 2 to 10 wt.% led to a significant 67% increase in flexural stress, particularly with ACN10, attributed to the effective dispersion of nanofillers within the HDPE matrix. CNT fillers enhanced the flexural stress by 36% but not as high as ACN fillers. A likely reason is CNT's long high aspect ratio structures that lead to structural entanglement.

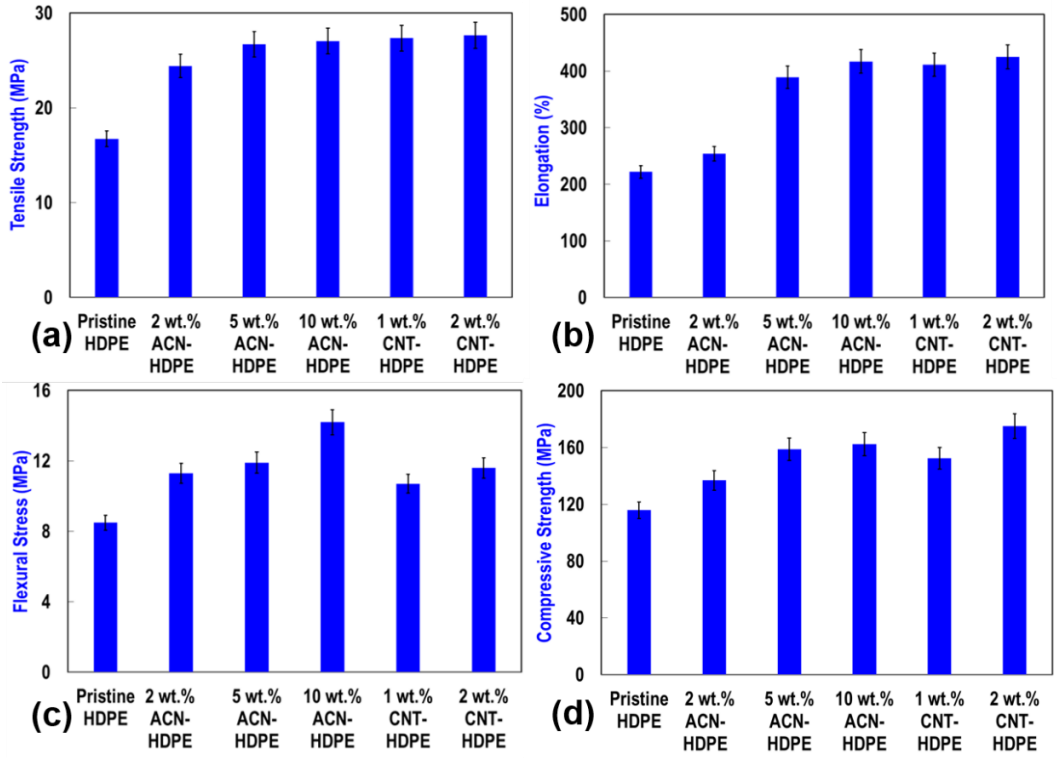

Figure 4. (a) Ultimate Tensile Strength, (b) Elongation at break, (c) Flexural Stress, and (d) Compression Stress of pristine HDPE, ACN-HDPE and CNT-HDPE nanocomposites

3.3.4 Compressive Strength

The compressive strength test measures a material's ability to withstand compressive forces, a crucial property for load-bearing construction materials. Enhancing the compressive strength of high-density polyethylene (HDPE) with nanofiller reinforcement expands its potential for advanced building materials. Figure 4(d) shows that increasing the nanofiller content in HDPE composites (ACN and CNT) improves compressive strength. ACN-HDPE composites with 10 wt.% ACN (ACN10) show a 41% increase, while CNT-HDPE composites with 2 wt.% CNT (CNT2) exhibits the highest enhancement, a 51% increase. These composites achieve compressive strengths over 150 MPa, far surpassing conventional materials like clay bricks (7.5 MPa) and mud bricks (4.4–18 MPa), making them suitable for load-bearing applications [36]. The enhancement is due to the high aspect ratio and mechanical properties of ACN and CNT fillers, which improve load distribution, crack-bridging, and stress transfer, increasing rigidity and stiffness. Optimal filler loadings (5-10 wt% for ACN, 1-2 wt% for CNT) maximize reinforcement efficiency, but excessive fillers can cause agglomeration and reduce performance. In conclusion, nanofiller-reinforced HDPE composites, particularly ACN10 and CNT2, offer significant improvements in compressive strength, sustainability, and cost-effectiveness, positioning them as promising alternatives to traditional construction materials. Future research will focus on optimizing filler dispersion and loadings for enhanced performance and long-term durability in construction.

3.3.5 Impact Strength

The impact strength, which measures a material's ability to absorb energy during fracture, increased significantly with higher nanofiller loadings of ACN and CNT in HDPE nanocomposites. As shown in Table 3, CNT-HDPE composites exhibited more significant improvements, with CNT2 showing the highest performance. These composites achieved a 194% increase in impact strength compared to pristine HDPE, demonstrating exceptional energy absorption and resilience without fracture under high loads. ACN-HDPE composites with 10 wt.% ACN (ACN10) also showed a 161% improvement in impact strength, remaining intact under extreme loading. The enhanced impact resistance of CNT2 and ACN10 can be attributed to the tortuous pathways created by the nanofillers, which dissipate impact energy, reducing crack initiation and

propagation. The high aspect ratio and superior interfacial bonding of CNTs enhance energy transfer and absorption, contributing to their superior performance over ACN fillers.

Table 3. Impact strength analysis on carbon-HDPE nanocomposites

Carbon HDPE nanocomposites	Impact Strength (unnotched) (kJ/m²)	Impact Strength (notched) (kJ/m²)
PT	8.9	5.9
ACN2	11.0	6.1
ACN5	13.7	8.0
ACN10	did not break	15.5
CNT1	did not break	17.2
CNT2	did not break	17.4

3.4 Flammability Analysis

Flammability analysis is crucial before constructing complex tall structures that must be fire-safe and stable.

3.4.1 Relative flammability

Figure 5(a) compares the flammability performance of pristine HDPE with reinforced HDPE nanocomposites via the vertical burning test. Despite its high flash ignition temperature, Pristine HDPE has potential fire hazards and fails within 40 seconds of ignition. Nanocomposites with increased carbon content showed improved burning times, with ACN10 and CNT2 lasting up to 77 to 87 s. Thus, ACN10, CNT1, and CNT2 demonstrated controlled dripping and self-extinguishing properties. The improvement is attributed to the carbon nanofillers, which form a char barrier that provides thermal insulation and enhances flame retardancy [37].

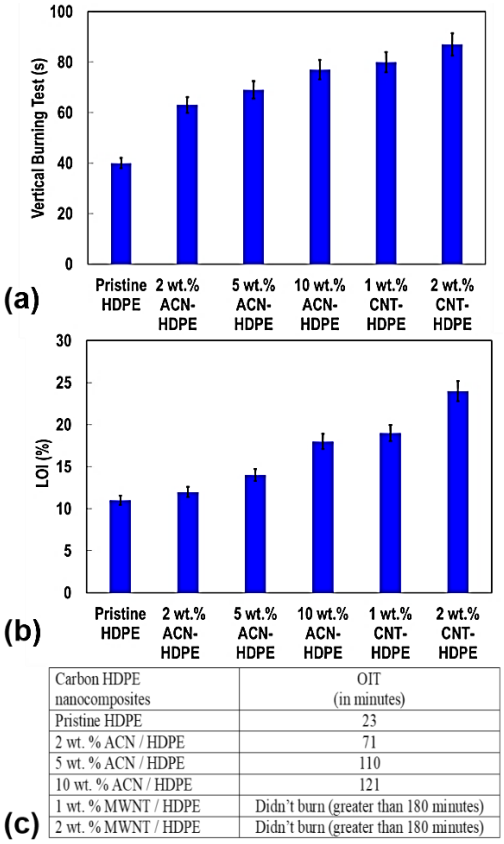

(c)

Carbon HDPE nanocomposites	OIT (in minutes)
Pristine HDPE	23
2 wt. % ACN / HDPE	71
5 wt. % ACN / HDPE	110
10 wt. % ACN / HDPE	121
1 wt. % MWNT / HDPE	Didn't burn (greater than 180 minutes)
2 wt. % MWNT / HDPE	Didn't burn (greater than 180 minutes)

Figure 5. (a) Relative flammability (using vertical burning test), (b) limiting oxygen index (LOI), and (c) OIT measurement of pristine HDPE against ACN-HDPE and CNT-HDPE nanocomposite specimens

3.4.2 Limiting Oxygen Index

The Limiting Oxygen Index (LOI) measures the minimum oxygen concentration required to sustain a flame on thermoplastic materials, which is crucial for assessing flammability risks in building construction [38] and provides a qualitative measure of a material's fire hazard reduction capabilities. Figure 5(b) shows that pristine HDPE (PT) had the lowest LOI value, needing only 11% oxygen to sustain combustion. ACN10 and CNT1 required 18% oxygen, a 63% increase compared to PT. CNT2 had the highest LOI value of 24%, indicating superior flame retardancy. Despite this, ACN10 also demonstrated significant flame retardancy, making it suitable for sheaths and cables in building frameworks and tunnels, reducing fire hazards. Incorporating ACN and CNT into HDPE enhances char formation during a fire, raising the LOI percentages. Char formation consumes combustible volatiles, increasing the oxygen required to sustain combustion [39]. These nanocomposites could help manufacture electrical connections in buildings and improve safety standards.

3.4.3 Thermal and Flammable Stability by Oxidation Induction Time (OIT)

Oxidative Induction Time (OIT) is crucial for assessing the oxidative stability and longevity of polymer materials in construction. A longer OIT indicates better stability. Figure 5(c) indicates that pristine HDPE (PT) had a low OIT of 21 s. In contrast, ACN-HDPE nanocomposites exhibited longer OITs as ACN filler content increased from 2 wt.% to 10 wt.%. ACN10 offered significant flame resistance with an OIT of 121 min, making it a viable construction material. CNT1 and CNT2 showed even higher stability, with OITs exceeding 180 min, highlighting their exceptional flame-retardant properties.

3.5 Weatherability Testing

Weather resistance is crucial for the durability and lifespan of construction materials. Extreme temperatures, UV radiation, moisture, wind, and pollutants can degrade materials over time. Choosing materials with strong weather resistance ensures buildings' longevity and structural integrity, making them more resilient and sustainable. Materials that endure prolonged exposure to harsh conditions without losing functionality are essential for constructing durable buildings.

3.5.1 Accelerated Ageing Test

The aging test schedule for CNT-HDPE and ACN-HDPE nanocomposites included UV exposure periods, reflecting their potential use in building materials like flooring, tiles, doors, windows, and waterproofing roofs. All specimens retained over 50% strength after UV exposure, with ACN10 and CNT2 showing the highest retention at 11.5% and 13.4% higher than pristine HDPE (Table 2). Pristine HDPE had low tensile strength retention due to photochemical degradation. Still, the addition of nanofillers improved its barrier properties [40], creating a longer path that inhibited UV light penetration and protected the polymer matrix from photo-degradation [41]. The current study predicts 1.5 years of outdoor exposure. However, a more in-depth aging test and further improvement are desired. Future work can focus on further optimizing filler dispersion and undergoing weather resistance tests for longer durations, up to 2000 hours, to further enhance the practical utility.

3.5.2 Environmental Stress Cracking Resistance

Table 4 shows that PT experienced slow crack growth, failing quasi-brittle at 50 hours, likely due to polymer chain folding, as seen in Figure 1 SEM micrographs. PT's low-stress levels suggest it could benefit from binding fillers or additives. ACN5 had the best performance, with a 50% failure point (F50) at 70 hours, while ACN2, ACN10, and CNT2 failed sooner. CNT1 also reached 70 hours before failing. ACN5 and CNT1 outperformed PT and other composites, achieving over 70 hours of Environmental Stress Crack Resistance (ESCR). However, higher filler loadings in ACN10 and CNT2 may have led to agglomeration and stress concentration, reducing resistance to environmental stress cracking. High nanofiller loadings can hinder the polymer matrix's ability to bridge and arrest cracks, potentially causing interfacial debonding and crack initiation [42]. In summary, PT failed to reach the 50% failure point within 60 h due to polymer chain folding, highlighting the need for binding fillers or additives. In contrast, ACN5 and CNT1 showed improved resistance to slow cracking, making them suitable construction materials. This enhanced performance is due to the optimal concentration and high aspect ratio structures of ACN and CNT fillers that improve load distribution and promote better crack-bridging within the HDPE composite.

3.5.3 Gas Permeability

Figure 6 reveals that pristine HDPE exhibits consistently high gas permeation, while ACN and CNT fillers significantly reduce the oxygen transmission rates (OTR) due to their barrier properties. There is an overall increasing trend in gas transmission rates until the 13th day, with ACN10 and CNT2 showing a 47% to 52% improvement over pristine HDPE. After the 14th day, all samples show lower OTR due to pore saturation. By the 31st day, CNT2 achieved the lowest permeability at 0.83 μL/s, compared to 2.9 μL/s for pristine HDPE, and ACN10 recorded a reduction to 1.15 μL/s. The weather ability test indicates that the nanofillers act as nodal points within the polymer matrix, delaying aging-related degradation and enhancing the long-term durability of the composite material.

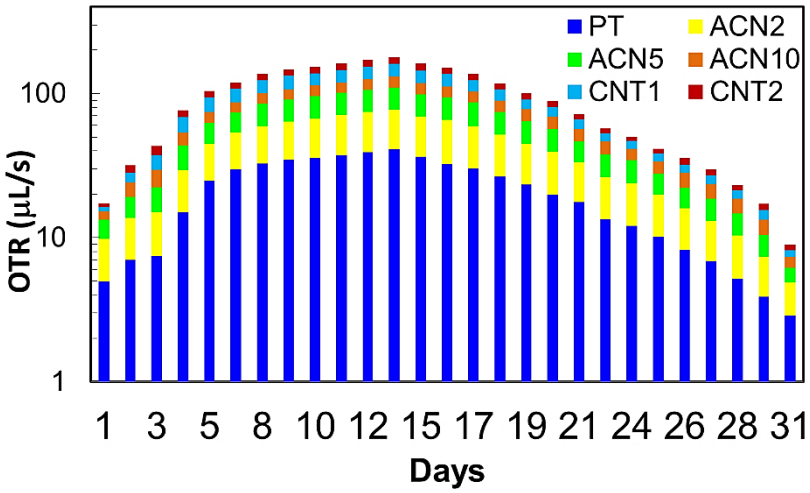

Figure 6. Oxygen permeability rate (OTR) comparison between pristine HDPE and carbon filler-based HDPE nanocomposites at various filler content over 31 days

Table 4. Weatherability test of ACN-HDPE and CNT-HDPE nanocomposites

Carbon HDPE nanocomposites	Tensile Strength Retention (after 500 h of UV exposure) (%)	ESCR Failure Point of samples at 50%
PT	52	Failed after 60 h
ACN2	55	Satisfactory after 48 h
ACN5	57	Satisfactory after 70 h
ACN10	58	Failed after 48 h
CNT1	58	Failed after 70 h
CNT2	59	Failed after 50 h

Table 5. Comparison of rate of decrease in oxygen transmission rate for HDPE composites vs. pristine HDPE

Sample	Day 1 (μL/s)	Peak Value (Day 13)	Reduction vs PT (%)
PT (HDPE)	5.00	40.9	-
ACN2	4.84	36.18	11.5%
ACN5	3.46	33.18	18.9%
ACN10	2.04	21.67	47%
CNT1	1.00	28.59	30.1%
CNT2	1.00	19.55	52.2%

3.6 Performance Comparison of ACN with CNT Nanofillers

Testing building materials is crucial for enhancing their performance and quality. ACN10 and CNT2 samples showed the most promising results among the tested materials. Notably, CNTs exhibit superior

properties even at lower filler concentrations than ACN. The study, summarized in Table 6, compares how different concentrations of CNT and ACN fillers influence the physical properties of HDPE nanocomposites used in building materials.

Thermal Property – ACN fillers exhibited better dispersion within the HDPE matrix, resulting in more homogeneous composite structures and reduced thermal boundary resistance compared to CNTs. The higher loading of ACN (10 wt.%) facilitated the formation of interconnected networks within the matrix, enabling continuous heat conduction pathways.

Both 10 wt.% ACN and 2 wt.% CNT nanofillers significantly improved the heat deflection temperature (HDT) and Vicat softening temperature (VST), increasing HDT by 51–52% and VST by 40%. These enhancements are attributed to the higher crystallinity and rigidity imparted by the nanofillers. In construction, these composites offer excellent structural integrity and can withstand elevated temperatures, making them suitable for high-performance applications.

Mechanical property - CNTs offer exceptional tensile strength, impact resistance, and compressive strength. As discussed in Section 3.3, adding just 1-2% CNTs significantly enhances the mechanical properties of CNT-HDPE composites. In contrast, ACN fillers at lower concentrations (less than 5 wt%) show minimal improvement. This difference is due to CNTs' high aspect ratio, which facilitates superior stress transfer and strong interfacial interactions with the polymer matrix. However, increasing ACN filler content to 5-10 wt% results in similar mechanical improvements attributed to ACN's high surface area. It's important to note that higher CNT concentrations can lead to agglomeration due to strong van der Waals interactions, causing poor dispersion in the HDPE matrix and degrading physical properties. Overall, the ACN10-HDPE composite shows potential for foundational construction applications, including flooring, railings, fences, and furniture.

Flammability – CNT2 and ACN10 fillers enhance the flammability resistance of HDPE nanocomposites due to their thermal stability and ability to form a protective char layer during combustion. Tests show that ACN10 and CNT2 achieve 72% to 118% impressively high improvements in LOI and relative flammability compared to pristine HDPE (PT). However, additional flame retardants may be essential for enhanced flame resistance in building applications.

Weatherability – The ESCR test, which assesses a material's resistance to cracking under harsh conditions (e.g., rain and acid rain), showed excellent performance for ACN-HDPE composites. After 504 hours of UV exposure, all composites retained more than 50% of their tensile strength, with ACN10 and CNT2 showing 12–14% higher retention than pristine HDPE.

The gas permeability test revealed that CNT-loaded HDPE outperforms ACN composites in oxygen barrier properties, achieving a 71.3% improvement over pristine HDPE at a lower filler loading (2 wt.%). Increasing ACN content to 10 wt.% resulted in a 60.3% improvement.

The reduction in gas permeability with CNT and ACN nanofillers is attributed to their high surface area and nano-dimensional heterostructures, which act as physical barriers. These fillers create tortuous diffusion pathways, forcing gas molecules to navigate around them. High-aspect-ratio CNTs, even at low filler contents, and ACNs at higher loadings significantly increase the complexity and length of diffusion paths, effectively reducing gas transmission.

ACN-HDPE vs. CNT-HDPE – ACN filler could match the performance of CNT-HDPE, but only at higher filler content. ACN filler offers advantages such as lower cost and high yield from abundant natural sources. In contrast, CNT fillers are limited by their complex and expensive production processes, which affect their scalability and overall practical use in polymer nanocomposites. A cost analysis of these two formulations of HDPE composites at 2 wt.% CNT and 10 wt.% ACN indicates approximately 40% cost savings towards developing the ACN-HDPE nanocomposites with 10 wt.% filler loading. This reflects the prospects of replacing the CNT-HDPE composites with the ACN-HDPE at 10 wt.% filler loading for various functional applications, including building construction.

Table 6. Property comparison of pristine HDPE with 10 wt. % ACN-HDPE and 2 wt. % CNT-HDPE

S. no.	Property	Units	Pristine HDPE	10 wt.% ACN-HDPE	% increase	2 wt.% CNT-HDPE	% increase
			Thermal property				
1	Thermal conductivity	W/mK	0.16	0.247	**46%**	0.224	**38%**
2	HDT	°C	72	108.9	**51.3**	110	**52.8**
3	VST	°C	67	93	**38.8**	97.4	**45.3**
			Mechanical property				
4	Tensile Strength	MPa	16.7	27.0	**61.6**	27.6	**65.3**
5	Elongation	%	222	417	**87.8**	425	**91.4**
6	Flexural stress	MPa	8.5	14.2	**67.3**	11.6	**36.6**
7	Compressive Strength	MPa	115	162.3	**41.1**	175.1	**52.3**
8	Impact strength	kJ/m²	5.9	15.5	**161.1**	17.4	**194.1**
			Flammability analysis				
9	Limiting Oxygen Index (LOI)	%	11	19	**72.7**	24	**118.2**
10	Relative Flammability	s	40	77	**92.5**	87	**117.5**
11	Thermal Stability by Oxidation (OIT)	min	23	121	**426.1**	Greater than 180 min	**628.3**
			Weatherability				
12	Tensile Strength Retention (after 500 h of UV exposure)	%	52	58	**11.5**	59	**13.5**
13	ESCR Failure Point of samples at 50%		Failed after 50h	Failed after 48 h	**-**	Failed after 50 h	**-**
14	OTR	uL/s	2.9	1.15	**60.3 (decrease)**	0.83	**71.3 (decrease)**

A comparison with existing studies on HDPE composites, summarized in Table 7, highlights the superior performance of the present study's ACN10 and CNT2 formulations. The key observations include a significant 62% improvement in tensile strength, outperforming many other fillers, including carbon black and CNT. The only composite with hybrid inorganic fillers, including 25% $CaCO_3$ microfilter + 1 wt.% fumed silica nanofiller, surpasses the present study with an exceptional 127% improvement in tensile strength. The present study achieves a 67% enhancement, exceeding reported carbon black and CNT composites but slightly below the $CaCO_3$ + silica formulation, which reaches an 86% improvement. However, a 161% enhancement in impact

strength in the present study is unmatched across all the listed composites, making it particularly suitable for applications requiring high-impact resistance. Other fillers, such as carbon black, CNT, and biochar, show only modest improvements ranging from 11.2% to 40%.

Overall, the ACN10 formulation provides balanced and superior physical property enhancements, demonstrating the efficacy of natural fillers at moderate loading levels.

Although inorganic $CaCO_3$ microfilter increases the tensile strength of HDPE composites, it reduces their impact resistance, especially at higher filler loadings where the brittle nature of $CaCO_3$ may lead to poor energy absorption under impact.

Table 7. Comparison of physical parameters of various carbon and other inorganic fillers incorporated with HDPE polymer

HDPE nanocomposites	**Percentage change in physical property concerning pristine HDPE**					
Optimum formulation of fillers	**Tensile strength (MPa)**	**Flexural strength (MPa)**	**Impact strength (kJ/m²)**	**WVTR (gm/m²-day)**	**OTR (gm/m²-day)**	**Ref.**
1 wt.% Carbon black			13% ↑	17.8% ↓	11.2% ↓	[30]
1 wt.% CNT				23.6% ↓	18.5% ↓	[30]
2 wt.% to 6 wt.% CNT	18% ↑	-	-	-	-	[24]
25% $CaCO_3$ microfiller + 1 wt.% fumed silica nanofiller	127% ↑	86% ↑	16.6% ↑	-	-	[32]
5 wt.% to 15 wt.% fly ash	3% ↑	-	-	-	-	[14]
2 wt.% to 20 wt.% carbon black	57.8% ↑	59.7% ↑	29.9% ↑			[11]
4wt.% to 6wt.% biochar of olive tree pruning	37.8% ↑	35.9% ↑	28.5% ↑	-	-	[29]
1 wt.% carbon black, nanodiamonds, fullerene, and CNT fillers	-	-	30-40% ↑	-	-	[31]
1 wt.% graphene and rGO	-	-	25-30% ↓			[31]
Present study 10 wt.% activated nanocarbon	62% ↑	67% ↑	161% ↑			

Note : ↑ sign indicates increase; ↓ sign indicates decrease

4. Conclusion

This study demonstrates the effectiveness of incorporating ACN and CNT nanofillers into an HDPE matrix to enhance thermal, mechanical, weatherability, and flame-resistant properties. CNT-HDPE and ACN-HDPE composites showed significant improvements across all performance metrics compared to pristine HDPE. While CNTs measured superior in some features at lower filler content (2 wt.%) due to their extraordinary thermal and mechanical properties, the nano-dimensional form of ACN fillers at higher loading of 10 wt.% with high surface area hierarchical structures also boons in terms of cost, sustainability, and specific application needs. Specifically, the 10 wt.% ACN-reinforced HDPE offers enhanced thermal stability, mechanical strength, and resistance against fire and harsh weather, making them suitable for interior building materials in residential and commercial spaces. Their higher crystallinity enhanced weatherability, and reduced gas permeability further emphasize their suitability as durable, high-performance materials. While CNT-HDPE composites demonstrated superior flame resistance and oxidative stability, ACN-HDPE

composites provided a sustainable and economical alternative by reducing material costs by almost 40% and aligning with sustainable environmental goals. Overall, ACN-HDPE composites offer a balanced combination of enhanced performance, affordability, and sustainability, making them a promising candidate for advanced, eco-friendly interior building materials. Future research can focus on integrating recycled HDPE with the ACN fillers to optimize performance and sustainability further.

Acknowledgment

S.C. acknowledges the Indian Institute of Technology Madras, Physics Department, for the SEM facility. M. C. is thankful to CIPET, Orissa, India, for sample preparation. M. C., J. M., and R. N. thank Amity University Uttar Pradesh, India, for their research support.

Author's Contributions: M.C. is responsible for data curation, investigation, methodology, and writing original drafts. S.C.R. is responsible for data curation and reviewing & editing the manuscript. J.M. is responsible for reviewing & editing the manuscript. R. N. is responsible for conceptualization, project administration, data analysis, reviewing & editing the manuscript.

Funding: This research received no external funding.

Conflicts of interest or competing interests: The authors declare that they have no known competing financial interests or personal relationships that could have appeared to influence the work reported in this article.

References

[1] Casini, M. Advanced Building Construction Methods. Constr. 4.0, **2022**, 405–470. https://doi.org/10.1016/B978-0-12-821797-9.00006-4

[2] Agarwal, S.; Gupta, R. K. Plastics in Buildings and Construction. Appl. Plast. Eng. Handb., **2017**, 635–649. https://doi.org/10.1016/B978-0-323-39040-8.00030-4

[3] Rajaeifar, M. A.; Abdi, R.; Tabatabaei, M. Expanded Polystyrene Waste Application for Improving Biodiesel Environmental Performance Parameters from Life Cycle Assessment Point of View. Renew. Sustain. Energy Rev., **2017**, *74*, 278–298. https://doi.org/10.1016/j.rser.2017.02.032

[4] Almohana, A. I.; Abdulwahid, M. Y.; Galobardes, I.; Mushtaq, J.; Almojil, S. F. Producing Sustainable Concrete with Plastic Waste: A Review. Environ. Challenges, **2022**, *9*, 100626–100632. https://doi.org/10.1016/j.envc.2022.100626

[5] Gedik, A. A Review on the Evaluation of the Potential Utilization of Construction and Demolition Waste in Hot Mix Asphalt Pavements. Resour. Conserv. Recycl., **2020**, *161*, 104956–104967. https://doi.org/10.1016/j.resconrec.2020.104956

[6] Majid, F.; Safe, M.; Elghorba, M. Burst Behavior of CPVC Compared to HDPE Thermoplastic Polymer under a Controlled Internal Pressure. Procedia Struct. Integr., **2017**, *3*, 380–386. https://doi.org/10.1016/j.prostr.2017.04.041

[7] Feldman, D. Polymer Nanocomposites in Building, Construction. J. Macromol. Sci. Part A, **2014**, *51*(3), 203–209. https://doi.org/10.1080/10601325.2014.871948

[8] Correia Diogo, A. Polymers in Building and Construction. In Materials for Construction and Civil Engineering; Springer International Publishing: Cham, **2015**, 447–499. https://doi.org/10.1007/978-3-319-08236-310

[9] Grace, R. Plastics Thriving in Building & Construction. Plast. Eng., **2017**, *73*(3), 12–20. https://doi.org/10.1002/j.1941-9635.2017.tb01671.x

[10] Choudhury, M.; Singh Bindra, H.; Mittal, J.; Nayak, R. Evaluation of Mechanical Properties of Carbon HDPE Composites. Mater. Today Proc., **2021**, *47*, 6712–6718. https://doi.org/10.1016/j.matpr.2021.05.119

[11] Vidakis, N.; Petousis, M.; Michailidis, N.; Mountakis, N.; Argyros, A.; Spiridaki, M.; Moutsopoulou, A.; Papadakis, V.; Charitidis, C. High-Density Polyethylene/Carbon Black Composites in Material Extrusion Additive Manufacturing: Conductivity, Thermal, Rheological, and Mechanical Responses. Polymers (Basel)., **2023**, *15*(24), 4717–4737. https://doi.org/10.3390/polym15244717

[12] Zhang, Q.; Zhang, D.; Xu, H.; Lu, W.; Ren, X.; Cai, H.; Lei, H.; Huo, E.; Zhao, Y.; Qian, M.; et al. Biochar Filled High-Density Polyethylene Composites with Excellent Properties: Towards Maximizing the Utilization of Agricultural Wastes. Ind. Crops Prod., **2020**, *146*, 112185–112194. https://doi.org/10.1016/j.indcrop.2020.112185

[13] Wang, R.; Meng, T.; Zhang, B.; Chen, C.; Li, D. Preparation and Characterization of Activated Carbon/Ultra-high Molecular Weight Polyethylene Composites. Polym. Compos., **2021**, *42*(6), 2728–2736. https://doi.org/10.1002/pc.26008

[14] Alghamdi, M. N. Performance for Fly Ash Reinforced HDPE Composites over the Ageing of Material Components. Polymers (Basel)., **2022**, *14*(14), 2913–2924. https://doi.org/10.3390/polym14142913

[15] Svensson, S.; Åkesson, D.; Bohlén, M. Reprocessing of High-Density Polyethylene Reinforced with Carbon Nanotubes. J. Polym. Environ., **2020**, *28*(7), 1967–1973. https://doi.org/10.1007/s10924-020-01739-2

[16] Makableh, Y.; Bozeya, A.; Rawashdeh, T.; Alnasra, I.; Hammam, H. A. Investigation of the Mechanical and Thermal Stability of Ultra-High Molecular Weight Polyethylene by Using Amide-Multi-Walled Carbon Nanotubes as a Reinforcement Material. Adv. Nat. Sci. Nanosci. Nanotechnol., **2022**, *13* (1), 015011. https://doi.org/10.1088/2043-6262/ac5d59

[17] Sahu, S. K.; Badgayan, N. D.; Samanta, S.; Rama Sreekanth, P. S. Experimental Investigation on Multidimensional Carbon Nanofiller Reinforcement in HDPE: An Evaluation of Mechanical Performance. Mater. Today Proc., **2020**, *24*, 415–421. https://doi.org/10.1016/j.matpr.2020.04.293

[18] Rao, B. D.; Pradhan, A.; Sethi, K. K. Study of Wear Performance and Mechanical Properties of HDPE on Addition of CNT Fillers. Mater. Today Proc., **2022**, *62*, 7501–7508. https://doi.org/10.1016/j.matpr.2022.03.705

[19] Kumar, S.; Ramesh, M. R.; Doddamani, M.; Rangappa, S. M.; Siengchin, S. Mechanical Characterization of 3D Printed MWCNTs/HDPE Nanocomposites. Polym. Test., **2022**, *114*, 107703–107714. https://doi.org/10.1016/j.polymertesting.2022.107703

[20] Åkesson, D.; Ramamoorthy, S. K. L.; Bohlén, M.; Skrifvars, V.; Svensson, S.; Skrifvars, M. Thermo-oxidative Aging of High-density Polyethylene Reinforced with Multiwalled Carbon Nanotubes. J. Appl. Polym. Sci., **2021**, *138* (26), 1–8. https://doi.org/10.1002/app.50609

[21] Jaiswal, M.; Majumdar, N.; Kumar, R.; Mittal, J.; Jha, P. Graphene Based Nano Gas Sensors: Mechanistic Study. Adv. Nat. Sci. Nanosci. Nanotechnol., **2022**, *13*(4), 043002. https://doi.org/10.1088/2043-6262/aca022

[22] Dabees, S.; Elshalakany, A. B.; Tirth, V.; Kamel, B. M. Synthesis and Characterization Studies of High-Density Polyethylene -Based Nanocomposites with Enhanced Surface Energy, Tribological, and Electrical Properties. Polym. Test., **2021**, *98*, 107193–107205. https://doi.org/10.1016/j.polymertesting.2021.107193

[23] A., N.; Taha, M.; Ibrahim, A. M. M.; A. K., A. Role of Hybrid Nanofiller GNPs/Al2O3 on Enhancing the Mechanical and Tribological Performance of HDPE Composite. Sci. Rep., **2023**, *13*(1), 12447–12460. https://doi.org/10.1038/s41598-023-39172-9

[24] Okolo, C.; Rafique, R.; Iqbal, S. S.; Saharudin, M. S.; Inam, F. Carbon Nanotube Reinforced High Density Polyethylene Materials for Offshore Sheathing Applications. Molecules, **2020**, *25*(13), 2960–2973. https://doi.org/10.3390/molecules25132960

[25] Sayam, A.; Rahman, A. N. M. M.; Rahman, M. S.; Smriti, S. A.; Ahmed, F.; Rabbi, M. F.; Hossain, M.; Faruque, M. O. A Review on Carbon Fiber-Reinforced Hierarchical Composites: Mechanical Performance, Manufacturing Process, Structural Applications and Allied Challenges. Carbon Lett., **2022**, *32*(5), 1173–1205. https://doi.org/10.1007/s42823-022-00358-2

[26] Carroccio, S. C.; Scarfato, P.; Bruno, E.; Aprea, P.; Dintcheva, N. T.; Filippone, G. Impact of Nanoparticles on the Environmental Sustainability of Polymer Nanocomposites Based on Bioplastics or Recycled Plastics – A Review of Life-Cycle Assessment Studies. J. Clean. Prod., **2022**, *335*, 130322–130334. https://doi.org/10.1016/j.jclepro.2021.130322

[27] Lim, J.-V.; Bee, S.-T.; Tin Sin, L.; Ratnam, C. T.; Abdul Hamid, Z. A. A Review on the Synthesis, Properties, and Utilities of Functionalized Carbon Nanoparticles for Polymer Nanocomposites. Polymers (Basel)., **2021**, *13*(20), 3547–3592. https://doi.org/10.3390/polym13203547

[28] Nisar, M.; Thue, P. S.; Maghous, M. B.; Geshev, J.; Lima, E. C.; Einloft, S. Metal Activated Carbon as an Efficient Filler for High-density Polyethylene Nanocomposites. Polym. Compos., **2020**, *41*(8), 3184–3193. https://doi.org/10.1002/pc.25610

[29] Vidakis, N.; Petousis, M.; Kalderis, D.; Michailidis, N.; Maravelakis, E.; Saltas, V.; Bolanakis, N.; Papadakis, V.; Spiridaki, M.; Argyros, A. Reinforced HDPE with Optimized Biochar Content for Material Extrusion Additive Manufacturing: Morphological, Rheological, Electrical, and Thermomechanical Insights. Biochar, **2024**, *6*(1), 37–58. https://doi.org/10.1007/s42773-024-00314-5

[30] Gill, Y. Q.; Jin, J.; Song, M. Comparative Study of Carbon-Based Nanofillers for Improving the Properties of HDPE for Potential Applications in Food Tray Packaging. Polym. Polym. Compos., **2020**, *28*(8–9), 562–571. https://doi.org/10.1177/0967391119892091

[31] Rahmanian, V.; Galeski, A.; Rozanski, A. Polyethylene Nanocomposites with Carbon Nanofillers: Similarities and Differences and New Insight on Cavitation in Tensile Drawing. Macromolecules, **2024**, *57* (3), 1337–1353. https://doi.org/10.1021/acs.macromol.3c01755

[32] Alshammari, B. A.; Alenad, A. M.; Al-Mubaddel, F. S.; Alharbi, A. G.; Al-shehri, A. S.; Albalwi, H. A.; Alsuabie, F. M.; Fouad, H.; Mourad, A.-H. I. Impact of Hybrid Fillers on the Properties of High Density Polyethylene Based Composites. Polymers (Basel)., **2022**, *14*(16), 3427–3442. https://doi.org/10.3390/polym14163427

[33] Salah, N.; Alfawzan, A. M.; Saeed, A.; Alshahrie, A.; Allafi, W. Effective Reinforcements for Thermoplastics Based on Carbon Nanotubes of Oil Fly Ash. Sci. Rep., **2019**, *9*(1), 20288–202301. https://doi.org/10.1038/s41598-019-56777-1

[34] Yang, D. J.; Zhang, Q.; Chen, G.; Yoon, S. F.; Ahn, J.; Wang, S. G.; Zhou, Q.; Wang, Q.; Li, J. Q. Thermal Conductivity of Multiwalled Carbon Nanotubes. Phys. Rev. B, **2002**, *66*(16), 165440–165446. https://doi.org/10.1103/PhysRevB.66.165440

[35] Sikora, J. W.; Gajdoš, I.; Puszka, A. Polyethylene-Matrix Composites with Halloysite Nanotubes with Enhanced Physical/Thermal Properties. Polymers (Basel)., **2019**, *11*(5), 787–798. https://doi.org/10.3390/polym11050787

[36] Vatani Oskouei, A.; Afzali, M.; Madadipour, M. Experimental Investigation on Mud Bricks Reinforced with Natural Additives under Compressive and Tensile Tests. Constr. Build. Mater., **2017**, *142*, 137–147. https://doi.org/10.1016/j.conbuildmat.2017.03.065

[37] Yang, Y.; Díaz Palencia, J. L.; Wang, N.; Jiang, Y.; Wang, D.-Y. Nanocarbon-Based Flame Retardant Polymer Nanocomposites. Molecules, **2021**, *26*(15), 4670–4702. https://doi.org/10.3390/molecules26154670

[38] Willard, J. J.; Wondra, R. E. Quantitative Evaluation of Flame-Retardant Cotton Finishes by the Limiting-Oxygen Index (LOI) Technique. Text. Res. J., **1970**, *40*(3), 203–210. https://doi.org/10.1177/004051757004000301

[39] Al Sheheri, S. Z.; Al-Amshany, Z. M.; Al Sulami, Q. A.; Tashkandi, N. Y.; Hussein, M. A.; El-Shishtawy, R. M. The Preparation of Carbon Nanofillers and Their Role on the Performance of Variable Polymer Nanocomposites. Des. Monomers Polym., **2019**, *22*(1), 8–53. https://doi.org/10.1080/15685551.2019.1565664

[40] Shaikh, A. M.; Kubade, P. R. Effect of Nanofillers on Rolled Polymer Nanocomposites: A Review. Mater. Today Proc., **2023**, *In press*. https://doi.org/10.1016/j.matpr.2023.07.346

[41] Zotti, A.; Zuppolini, S.; Borriello, A.; Vinti, V.; Trinchillo, L.; Zarrelli, M. The Effect of Carbon-Based Nanofillers on Cryogenic Temperature Mechanical Properties of CFRPs. Polymers (Basel)., **2024**, *16*(5), 638–652. https://doi.org/10.3390/polym16050638

[42] Robeson, L. M. Environmental Stress Cracking: A Review. Polym. Eng. Sci., **2013**, *53*(3), 453–467. https://doi.org/10.1002/pen.23284